Available online at www.sciencedirect.com

jmr&t Journal of Materials Research and Technology

journal homepage: www.elsevier.com/locate/jmrt

Original Article

Effect of Ag_2O substituted in bioactive glasses: a synergistic relationship between antibacterial zone and radiation attenuation properties

H.O. Tekin [a], M.S. Al-Buriahi [b], Shams A.M. Issa [c,d], Hesham M.H. Zakaly [d,e,**], Bashar Issa [a], Imen Kebaili [f,g], Ali Badawi [h,j], M.K.A. Karim [i], K.A. Matori [i], M.H.M. Zaid [i,*]

[a] Department of Medical Diagnostic Imaging, College of Health Sciences, University of Sharjah, Sharjah, 27272, United Arab Emirates
[b] Department of Physics, Sakarya University, Sakarya, Turkey
[c] Department of Physics, Faculty of Science, University of Tabuk, Tabuk, Saudi Arabia
[d] Physics Department, Faculty of Science, Al-Azhar University, Assiut, 71452, Egypt
[e] Institute of Physics and Technology, Ural Federal University, Ekaterinburg, 620002, Russia
[f] Department of Physics, Faculty of Science, King Khalid University; P.O. Box 9004, Abha, Saudi Arabia
[g] Laboratoire de Physique Appliquée, Groupe de Physique des matériaux luminescents, Faculté des Sciences de Sfax, Département de Physique, Université de Sfax, BP 1171, Sfax, 3018, Tunisia
[h] Department of Physics, College of Science, Taif University, P.O. Box 11099, Taif, 21944, Saudi Arabia
[i] Department of Physics, Universiti Putra Malaysia, Serdang, Selangor, 43400, Malaysia
[j] Department of Physics, University College of Turabah, Taif University, P.O. Box 11099, Taif, 21944, Saudi Arabia

ARTICLE INFO

Article history:
Received 11 February 2021
Accepted 7 June 2021
Available online 15 June 2021

Keywords:
Bioactive glasses
Antibacterial properties
Radiation attenuation
MCNPX

ABSTRACT

In this study, a promising relationship between antibacterial zone and radiation attenuation properties was investigated in Ag_2O doped bioactive glasses with a chemical composition of $xAg_2O–20Li_2O–25TeO_2$-$(55-x)B_2O_3$ (where x = 0, 0.5, 1.0, 1.5, and 2.0 mol%). For this aim, a wide-ranging radiation attenuation characterization procedure was performed on Ag_2O substituted bioactive glasses. The general-purpose Monte Carlo code MCNPX (v.2.7.0) was used to model bioactive glasses. The mass attenuation coefficients were calculated using a gamma-ray transmission setup. The coefficients obtained were used to determine other important attenuation properties. Finally, for particular behaviors, exposure (EBF) and energy absorption (EABF) build-up factors were calculated for specific attitudes of Ag_2O substitutions in bioactive glasses during the interaction process. The results showed that there is direct relationship between Ag_2O substitution amount and radiation attenuation properties. In addition to its well-behaviors on inhibition zone against bacterial occurrences, it can be concluded that increasing Ag_2O would increase the gamma-ray attenuation properties of studied bioactive glass system.

* Corresponding author.
** Corresponding author.
E-mail addresses: h.m.zakaly@azhar.edu.eg (H.M.H. Zakaly), mhmzaid@upm.edu.my (M.H.M. Zaid).
https://doi.org/10.1016/j.jmrt.2021.06.025

1. Introduction

Bioactive glass is an amorphous structure composed of certain elements in the human body including silicone, calcium, sodium, phosphorous and oxygen [1]. Glass-ceramic and surface-reactive material based on biomaterials may be classified as bioactive glass [2]. In last decades, different testing methods have demonstrated that bioactive glasses are highly biocompatible. Consequently, their innovative material properties and biocompatibility in living biological systems have led them to further use in surgical restoration or replacement operations as candidate implant materials [3].

The property of bioactivity refers to the materials' ability to specifically bind to the bone and strengthen bone structure. The bioactivity level depends on the material's ability to provide a regulated and continuous supply of chemical indications to promote cell function and tissue growth. Chemical composition, crystalline structure and processing parameters of bioactive substances regulate the rate of development of new tissues and resorption of graft material [4]. A bioactive glass generally consists of silica or calcium-based structure [5]. A bioactive material induces a certain biological reaction at the material interface leading to a connection between the tissues and the material. On the other hand, biocompatibility of bioactive glasses is also an important issue that needs to be addressed [6]. As third generation biomaterials, bioactive glasses (BGs) can establish a more rapid interfacial link between implants and host tissue than other bio ceramics in the treatment of biological defects [7]. As other glassy materials, bioactive glasses have also different types of network formers such as SiO_2, B_2O_3 and P_2O_5. This type of network formers can form single component glasses. However, Ag_2O (silver oxide) is known as a promising glass network modifier with its remarkable biological properties. Beyond that, some of its antibacterial and anticancer properties also brought Ag_2O to the fore by sparking researchers' interest. The literature review showed that different types of studies focused on antibacterial properties of Ag_2O against several bacteria types. In this study, bioactive glasses are selected from a previous investigation by Naresh et al., [8]. Accordingly, we extended the concept of the fabricated glasses by determining the gamma-ray attenuation parameters. The concept of the source paper has encouraged us since the previous study focused on impact fog Ag_2O substitution on antibacterial, optical, structural properties. Since the bioactive materials have a promising role in medical applications, our investigation aimed to extend the studied properties by adding the radiation attenuation properties. Its well-known that any type of internal body material is a candidate to interact with medical radiation either with diagnostic or with therapeutic applications. Considering the use of bioactive glasses in the body, especially for hard tissues, their interaction with radiation is of particular importance. The absorption that occurs during the interaction of radiation with tissue directly affects the quantity of radiation during both treatment and diagnostic procedures, and closely concerns the possible clinical results. The antibacterial properties of Ag_2O have also raised the question of what kind of attitudes might exhibit during its use, especially when interacting with ionizing radiation. Therefore, this study aimed to investigate the variation of attenuation properties depending on Ag_2O additive amount. Since the initial results provided some remarkable advantages of Ag_2O additive in terms of antibacterial zone, attenuation behaviors of glasses with different reinforcement amount are worth investigating in detail. Following this concern, the wide-ranging radiation attenuation properties such as linear (LAC) and mass (MAC) attenuation coefficients, effective atomic numbers (Z_{eff}), mean free path (mfp), effective atomic weight for absorption, effective conductivity at 300 K for attenuation, half value layer, exposure (EBF) and energy absorption (EABF) build-up factors of some Ag_2O-doped bioactive glasses were investigated by using Monte Carlo method. The antibacterial zone's synergistic or semi-synergistic effect on radiation attenuation properties will be examined. For diagnostic and therapeutic radiation energies, the attenuation properties of various Ag_2O additive ranges that exhibit antibacterial properties will be discussed separately. Thus, examining the changes in radiation interaction properties as a function of the rate of Ag_2O additive and, in particular, tracking certain behaviors in certain energy ranges will contribute significantly to the medical radiation literature.

2. Methods and Materials

A series of bioactive glasses reinforced by Ag_2O additive with a chemical composition of $xAg_2O-20Li_2O-25TeO_2$-$(55-x)B_2O_3$ (where $x = 0$, 0.5, 1.0, 1.5, and 2.0 mol%) was investigated. The investigated glasses have been obtained from a previous successful investigation [8] on the antibacterial, optical, structural and impedance investigation of Ag-0, Ag-0.5, Ag-1, Ag-1.5, and Ag-2 glasses. This study, on the other hand, is a continuation and aims to examine the relationship between the existing outcomes on antibacterial zone improvements and radiation attenuation properties. The technical details of radiation attenuation properties and its characterization steps will be discussed with their technical details as well as highlights. In addition to Monte Carlo simulations, Py-MLBUF a promising web-based tool for determination of radiation attenuation properties for radiological protection and dosimetry purposes [9].

Monte Carlo simulations: To determine the mass attenuation coefficients of studied bioactive glasses, general purpose Monte Carlo code entitled MCNPX (version 2.7.0) [10] was successfully utilized. Fig. 1 shows the 3D view of MCNPX simulation setup for gamma ray transmission calculations. To begin, MCNPX input data was created using the key components such as cell cards, surface cards, and source data. In a Lead (Pb) shield block, a point isotropic source was discovered. The chemical concentrations (wt. percent) and samples densities (g/cm^3) of the bioactive glass specimens were then modelled [8]. The cylindrical geometry was used to create the outline of the glass specimen with 5 cm radius. Accordingly, the appropriate material properties were filled in along the edges of the constructed surfaces. (i.e. elemental mass fraction and material density) in cell card. The elemental mass fractions of investigated bioactive glasses can be seen from Table 1. It should be noted that elemental definition of glass

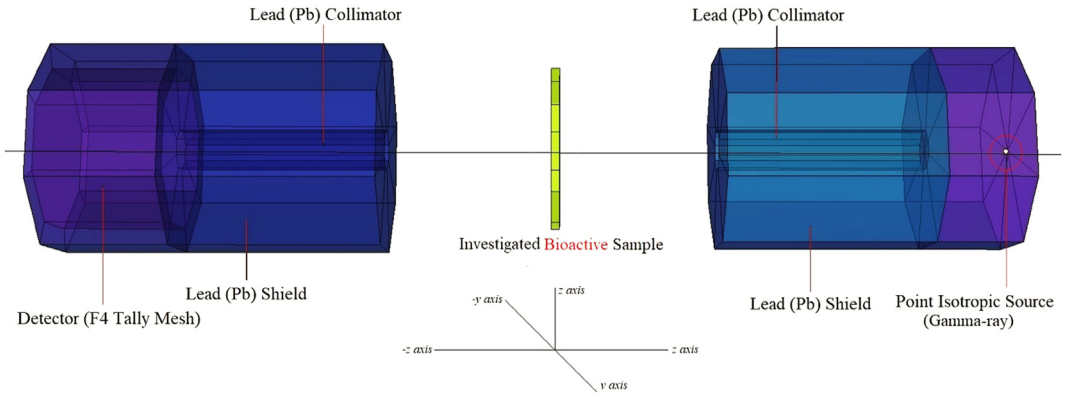

Fig. 1 – 3-D view of MCNPX simulation setup for gamma ray transmission calculations obtained from MCNPX Visual Editor (visedX22S).

specimens was created in *Mn* variable card. The value of interaction (IMP: p, e) for photon and electron interactions was calculated after the initial stage of cell description. In the MCNPX code, this can be described as a variance reduction technique. On the other hand, on the other side of the bioactive glass material, a detector field (F4 Tally Mesh) for counting attenuated (secondary) gamma rays was found. The average photon flux in a point or cell can be detected using this form of tally mesh. A Pb block shield was used to cover the detector field in order to capture dispersed gamma rays and improve detection performance. In the simulation, each run was repeated for 10^8 particles for each bioactive glass sample at different photon energies as shown in Table 2. The uncertainty of MCNPX was less than 1% for all simulations. One can find the details about the calculation procedures from our previous publications [11–16].

3. Results and discussion

Firstly, gamma attenuation properties of bioactive glasses reinforced by Ag_2O additive were evaluated using the Monte Carlo method illustrated by the basic transmission geometry in Fig. 1. Specifically, we estimated the gamma photons number passed a thin slab of the studied bioactive glasses. Thereafter, a mathematical approach namely Beer–Lambert law was utilizing to determine the linear attenuation coefficients (LAC) of the studied glasses. The variation of LAC with the energy (up to 15 MeV) for the bioactive glasses under study is shown in Fig. 2. Clearly, at both high and low energies, the maximum LAC was noted for the glass sample label as Ag-0. For all of the studied glasses (Ag-0, Ag-0.5, Ag-1, Ag-1.5, and Ag-2), the LAC values showed a decrease behavior as the energy increased. This reduction of LAC was a very sharp in the low energy region (below 2 MeV), while it was a soft in the high energy region (above 2 MeV). Furthermore, the highest LAC was observed at 15 keV with the values of 72.5, 61.1, 63.3, 66.1, and 68.7 for the bioactive glasses of Ag-0, Ag-0.5, Ag-1, Ag-1.5, and Ag-2, respectively. The minimum LAC was noted at 15 MeV with the values of 0.0930, 0.1313, 0.1324, 0.1335, and 0.1357 cm^{-1} for all the bioactive glass samples, respectively. The variation of LAC with the energy is attributed to the partial interactions of photon with absorbing target. For example, the photoelectric effect (PE) is the dominant interaction at the low energies, the Compton scattering (CS) dominates in the medium energies, and the pair production is the dominating process at the high energies [16]. Before going deep in discussion for the gamma attenuation properties of the studied bio glass system, we shall check the accuracy of the obtained simulation results for LAC. In this regards, the LAC values were converted into MAC values which can be compared with the outcomes of the XCOM software (theoretical calculation).

Table 1 – Elemental mass fractions (wt.%) of investigated bioactive glass samples.

Sample	Li	B	O	Te	Ag
Ag-0	0.03299	0.14129	0.44671	0.37901	0
Ag-0.5	0.03267	0.13867	0.44057	0.01269	0.37540
Ag-1	0.03236	0.13610	0.43454	0.02515	0.37185
Ag-1.5	0.03206	0.13358	0.42863	0.03737	0.36837
Ag-2	0.03176	0.13110	0.42282	0.04936	0.36495

Table 2 shows a comparison between the MAC values obtained from MCNP and XCOM for all of the studied glasses. Generally, the maximum Dev.% between MCNP and XCOM was less than 1.0% and this confirms our obtained results in the present work for the investigated bioactive glasses. The MAC of the present bioactive glasses at different concentrations of Ag_2O is depicted in Fig. 3. It is very clear that the general behavior of MAC is similar to that of LAC, however, the MAC as independent–density parameter is more useful than LAC for describing gamma attenuation of materials [17–20]. The highest MAC of the present glasses can be observed at 15 keV with the values of 20.1, 16.5, 17.0, 17.5, 17.9 cm^2/g for the bioactive glasses of Ag0, Ag0.5, Ag1, Ag1.5, and Ag2, respectively. In addition to demonstration of MAC values, a detailed comparison was done between the zone of inhibition (mm) for Samonella and MAC values at 0.015 MeV. The previous results showed that molar increment of Ag_2O in bioactive glass sample increased the zone of inhibition (mm) [8]. However, our results showed that Ag_2O additive amount has also a direct effect on mass attenuation coefficients. The synergistic behavior of MAC and zone of inhibition (mm) with

Table 2 – Mass attenuation coefficients of investigated bioactive glass samples obtained from XCOM and MCNPX.

Energy	Ag-0		Ag-0.5		Ag-1		Ag-1.5		Ag-2	
	XCOM	MCNPX	XCOM	MCNPX	XCOM	MCNPX	XCOM	MCNPX	XCOM	MCNPX
0.015	20.1420	20.2456	16.5360	16.6236	17.0140	17.1621	17.4830	17.5124	17.9440	17.625
0.02	9.3079	9.3154	7.6185	7.6326	7.8390	7.84122	8.0552	8.0824	8.2673	8.2682
0.0263	4.4567	4.4654	19.5700	19.6123	19.5230	19.5245	19.4780	19.5101	19.4330	19.4426
0.03	3.1896	3.1995	14.0700	14.1230	14.0350	14.0952	14.0010	14.0754	13.9670	13.9710
0.04	7.9725	7.9854	6.8590	6.8621	7.0532	7.1012	7.2437	7.3024	7.4305	7.4314
0.05	4.4634	4.4521	3.8129	3.8263	3.9203	3.9326	4.0256	4.0524	4.1289	4.1293
0.0595	2.8381	2.8399	2.4137	2.4230	2.4808	2.4816	2.5465	2.5514	2.6111	2.6134
0.06	2.7805	2.7921	2.3646	2.3710	2.4302	2.4328	2.4946	2.4953	2.5578	2.5582
0.08	1.3340	1.3354	1.1353	1.1406	1.1650	1.1674	1.1942	1.2016	1.2227	1.2230
0.1	0.7758	0.7801	0.6665	0.6671	0.6824	0.6851	0.6980	0.7046	0.7133	0.7136
0.15	0.3283	0.3294	0.2929	0.2932	0.2979	0.3001	0.3028	0.3054	0.3076	0.3079
0.2	0.2048	0.2051	0.1896	0.1912	0.1918	0.1924	0.1939	0.1941	0.1960	0.1962
0.3	0.1284	0.1290	0.1245	0.1248	0.1251	0.1263	0.1257	0.1263	0.1263	0.1265
0.4	0.1020	0.1024	0.1010	0.1014	0.1012	0.1016	0.1015	0.1024	0.1017	0.1025
0.5	0.0882	0.0896	0.0883	0.0886	0.0884	0.0891	0.0884	0.0898	0.0885	0.0899
0.6	0.0793	0.0798	0.0798	0.0802	0.0798	0.0803	0.0798	0.0812	0.0798	0.0813
0.662	0.0751	0.0763	0.0757	0.0760	0.0757	0.0761	0.0757	0.0763	0.0757	0.0764
0.8	0.0677	0.0684	0.0685	0.0689	0.0685	0.0691	0.0685	0.0689	0.0684	0.0688
1	0.0601	0.0623	0.0610	0.0615	0.0609	0.0616	0.0609	0.0612	0.0608	0.0612
1.173	0.0551	0.0563	0.0560	0.0564	0.0560	0.0565	0.0559	0.0561	0.0559	0.0563
1.333	0.0516	0.0524	0.0524	0.0531	0.0524	0.0532	0.0523	0.0526	0.0523	0.0528
1.5	0.0485	0.0493	0.0494	0.0496	0.0493	0.0496	0.0493	0.0495	0.0492	0.0497
2	0.0422	0.0436	0.0429	0.0432	0.0429	0.0433	0.0428	0.0432	0.0428	0.0433
2.506	0.0381	0.0392	0.0387	0.0390	0.0387	0.0392	0.0387	0.0391	0.0387	0.0393
3	0.0354	0.0366	0.0359	0.0363	0.0360	0.0364	0.0360	0.0362	0.0360	0.0363
4	0.0319	0.0325	0.0324	0.0326	0.0324	0.0325	0.0324	0.0325	0.0325	0.0327
5	0.0299	0.0306	0.0303	0.0309	0.0303	0.0312	0.0304	0.0309	0.0305	0.0310
6	0.0286	0.0291	0.0290	0.0292	0.0291	0.0295	0.0292	0.0295	0.0293	0.0296
8	0.0274	0.0279	0.0277	0.0281	0.0278	0.0283	0.0279	0.0282	0.0281	0.0283
10	0.0269	0.0274	0.0272	0.0275	0.0274	0.0276	0.0275	0.0276	0.0277	0.0278
15	0.0271	0.0276	0.0273	0.0277	0.0275	0.0279	0.0278	0.0280	0.0280	0.0282

increasing Ag_20 additive amount can be seen in Fig. 4. An increment trend in MAC values was reported from Ag-0 to Ag-2 sample. One can say that Ag_2O, as an additive material type for improvement of antibacterial zone of inhibition, can be a candidate material for mass attenuation coefficient improvement in the investigated energy level (MeV).

The MFP is an important term for gamma interaction calculations to describe the attenuation mechanism through materials [21–23]. The MFP of the present bioactive glasses as a function of energy (wide energy range up to 15 MeV) is depicted in Fig. 5. Obviously, the MFP values start very small at the low energy region with the value about 0.015 cm for all of

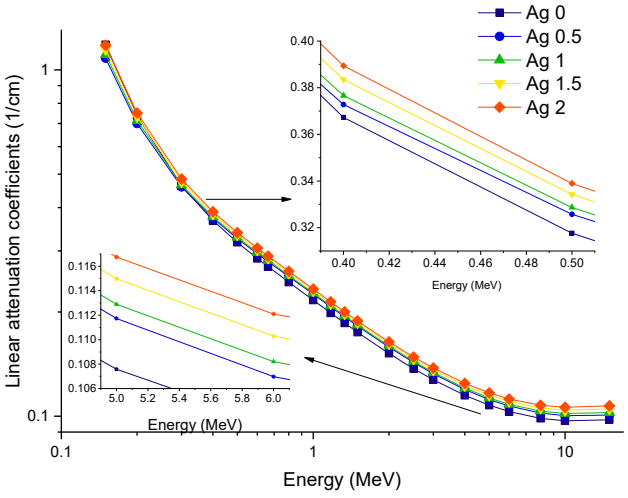

Fig. 2 – Variation of linear attenuation coefficients (LAC) of Ag0, Ag0.5, Ag1, Ag1.5 and Ag2 bioactive glasses as a function of incident photon energy (MeV).

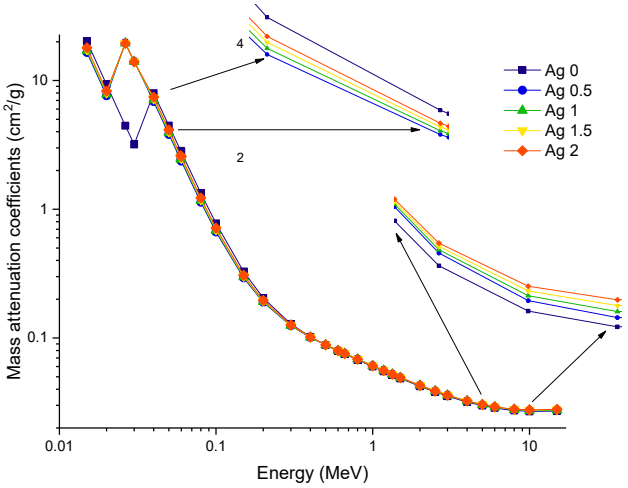

Fig. 3 – Variation of mass attenuation coefficient (MAC) of Ag0, Ag0.5, Ag1, Ag1.5 and Ag2 bioactive glasses as a function of incident photon energy (MeV).

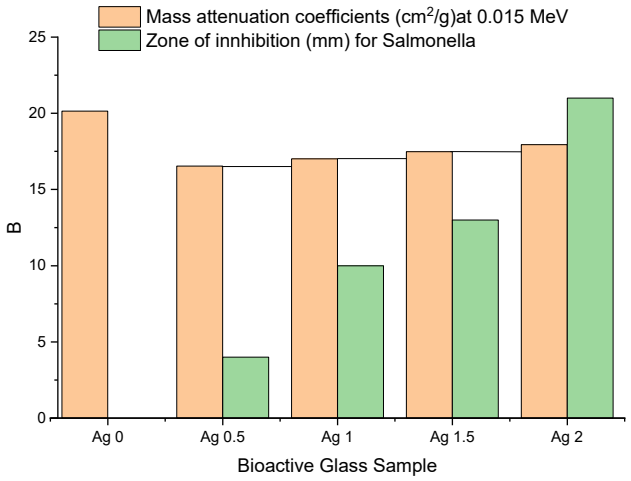

Fig. 4 – A comparative demonstration between antibacterial zone of inhibition and mass attenuation coefficients of Ag0, Ag0.5, Ag1, Ag1.5 and Ag2 bioactive glasses.

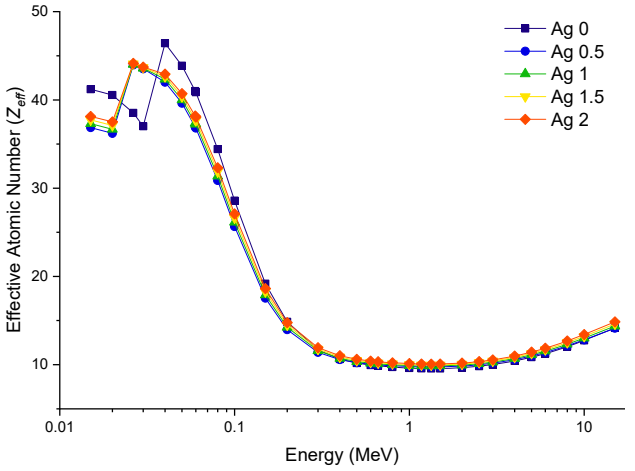

Fig. 6 – Variation of effective atomic number (Zeff) of Ag0, Ag0.5, Ag1, Ag1.5 and Ag2 bioactive glasses as a function of incident photon energy (MeV).

the present glasses. Thereafter, with the increase energy the MFP values of the present glasses increased swiftly reaching the value of 10.2 cm at 15 MeV for the bioactive glass sample of Ag-0. Such behavior is standard and well-known for the photon interaction with matter [24]. Effective atomic number (EAN) which associated with the partial attenuation process of photons, is useful to test suitability of a material for gamma applications [25–27]. Over a wide range of energies from 15 keV to 15 MeV, the EAN of the present bioactive glasses as a function of energy is depicted in Fig. 6. We found that the maximum EAN was noted at 40 keV with the value of 46.5 for the Ag-0 bioactive glass, however, the maximum EAN values for the remaining samples were observed at 26 keV with the value around 44.0. Effective atomic weight (A_{eff}) is a key parameter to understand the interaction process between the material and radiation considering the atomic weight. Similar to EAN, effective atomic weight of compound or composite specimen can be explained by a single-value [28]. This concept has inspired us to consider the mechanism of radiation interaction of bioactive glasses with atomic weight.

Fig. 7 shows the variation of A_{eff} against photon energy (MeV). We found that the effective atomic weight (A_{eff}) varied from 20.5281 g/mol to 21.3220 g/mol. Consequently, the lowest A_{eff} was reported for Ag-0 sample whereas the highest for Ag-2 sample. Effective conductivity is known as a material feature that explains the capability to conduct heat. Fig. 8 displays that effective conductivity values of the studied bioactive glasses were changed with incoming photon energy. On the other hand, effective conductivity at 300 K for attenuation is increased with Ag_20 substation amount in the bioactive glass. Obviously, it can be seen from Fig. 8 that Ag-2 sample with highest level of Ag_2O concentration additive has maximum conductivity almost at all energy values. It can be said that, increasing Ag_2O concentration additive can also be useful for further improvements in the conductivity of the bioactive

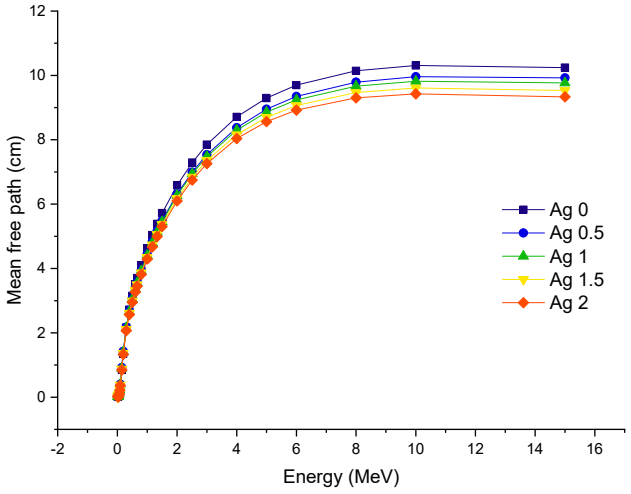

Fig. 5 – Variation of mean free path (mfp) of Ag0, Ag0.5, Ag1, Ag1.5 and Ag2 bioactive glasses as a function of incident photon energy (MeV).

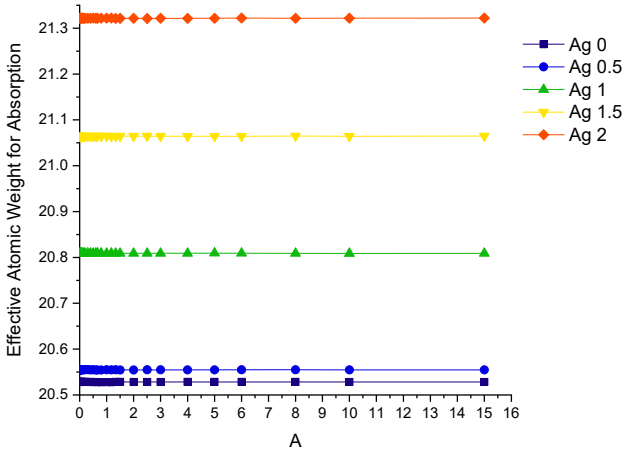

Fig. 7 – Variation of effective atomic weight of Ag0, Ag0.5, Ag1, Ag1.5 and Ag2 bioactive glasses as a function of incident photon energy (MeV).

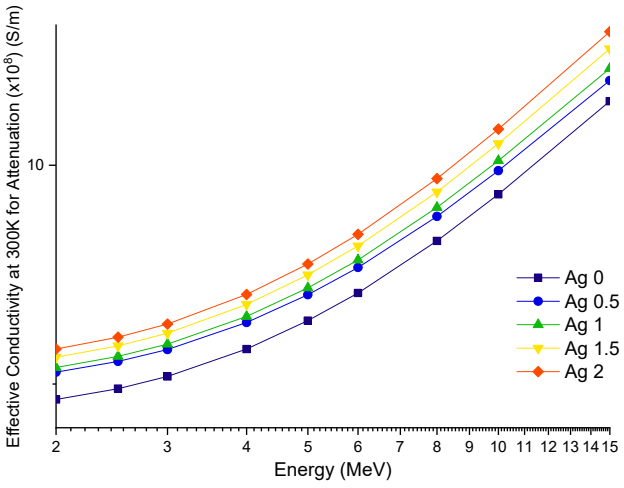

Fig. 8 – Variation of effective conductivity of Ag0, Ag0.5, Ag1, Ag1.5 and Ag2 bioactive glasses as a function of incident photon energy (MeV) at 300 K.

glass materials. It is should mention that the attenuation parameters of different types of glasses (bioactive glasses, bioactive glasses and bioceramics) will change (increase or decrease) by substituting the concentrations of constituents oxides of glass [29–31]. For example, the substitution of heavy oxide by light one leads to decrease the attenuation ability of glass and via versa. Therefore, in the present work, we found that the attenuation ability slightly decreases under the substitution of B_2O_3 by Ag_2O. In the medical applications, knowing the gamma buildup factors, especially the one associated with the exposure rate, gives a detailed information about absorbed dose in the medium.

Separately for every bioactive glass specimen, the exposure buildup factor (EBF) over a wide range of the penetration depths varying from 0.5 to 40 mfp were calculated and then the obtained results are plotted in Fig. 9 (a–e). According to these figures, there are three explicit regions of EBF versus photon energy at the different penetration depths up to 40 mfp. Such regions are basically relevant to the partial photon interactions with matter. In the first region, the appeared peaks due to the photoelectric phenomenon near the binding energy of the high atomic number elements. Thereafter, the region of Compton phenomenon where the EBF values were almost constant. Finally, the third region is relevant to the pair production where the EBF showed a slight increase due to the absorption processes. The EBF for all the present bioactive glasses at 10 mfp and for energies up to 15 MeV is shown in Fig. 10. This figure exhibited the influence of Ag_2O on the EBF and then on the absorbed dose. Such that the sample Ag-2 (high Ag_2O concentration) possesses the highest EBF among the studied bioactive glasses. For example, we found that at 10 mfp and incident energy of 1 MeV the EBF were 11.0691, 12.1098, 12.2364, 11.6638, and 11.7685 for the bioactive glasses of Ag0, Ag0.5, Ag1, Ag1.5, and Ag2, respectively.

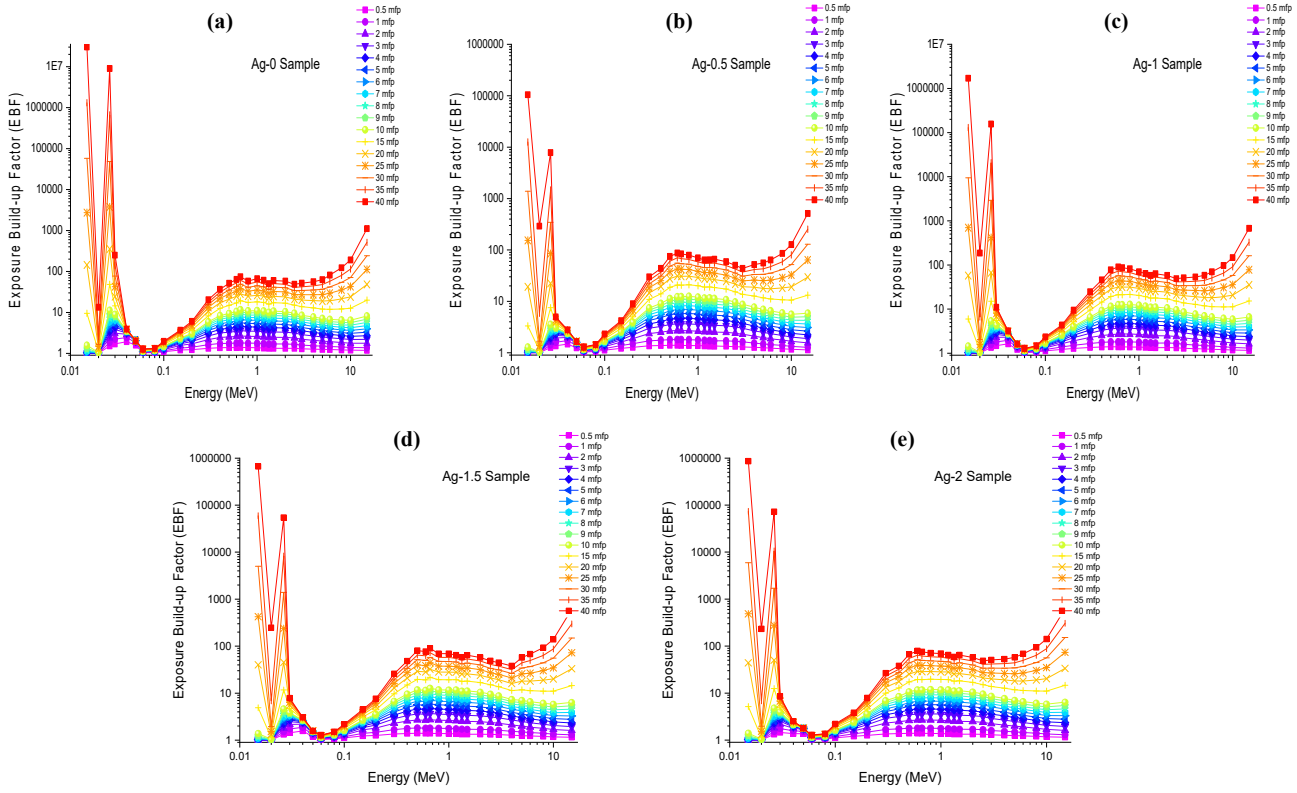

Fig. 9 – Variations of exposure buildup factor (EBF) of Ag0, Ag0.5, Ag1, Ag1.5 and Ag2 bioactive glasses as a function of incident photon energy (MeV) at different mean free path values (1–40 mfp).

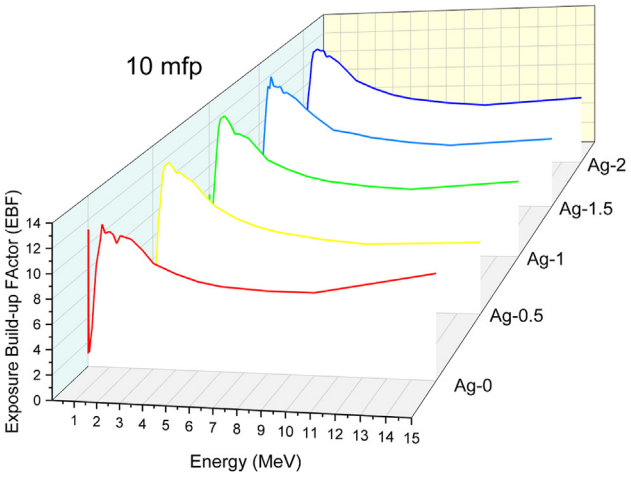

Fig. 10 – Variations of exposure buildup factor (EBF) of Ag0, Ag0.5, Ag1, Ag1.5 and Ag2 bioactive glasses as a function of incident photon energy (MeV) at 10 mfp.

4. Conclusion

Hench et al. discovered bioactive glasses in 1969. They are a class of reactive materials capable of bonding to mineralized bone tissue in a physiological environment. In the biomedical sector, bioactive glasses are commonly used. Initially, bioactive glasses were used in the form of solid pieces to replace small bones in middle ear surgery. Later, several applications of bioactive glasses, including the dental region, have been suggested. Recent years have seen a surge in interest in bioactive glasses and their potential applications in tissue engineering and regenerative medicine. The extensive applications of bioactive materials in the medicine have encouraged us to perform a study on some bioactive samples that previously investigated in terms of Ag_2O substitution and antibacterial properties. Accordingly, a promising relationship between antibacterial zone and radiation attenuation properties was investigated in Ag_2O doped bioactive glasses with a chemical composition of $xAg_2O–20Li_2O–25TeO_2$-(55-x) B_2O_3 (where x; 0-0.5-1-1.5 and %2 mol). A previous investigation was used for comprehensive investigation and potential synergistic effect between the antibacterial zone improvements and radiation attenuation properties depending on Ag_2O additive amount. The importance of bioactive glasses for medical purposes is apparent in the literature. Their promising properties and wide-range utilization aims in human body gives them a well-deserved reputation as a biomaterial. The previous results showed that Ag_20 is a superb additive type to increase the antibacterial zone against some types of bacteria. Considering the obtained results in our investigation, it can be concluded that Ag_20 has also a direct impact on radiation attenuation properties on bioactive glasses. It is and obvious fact that bioactive glasses can be used for replacement of biological structures. Therefore, it is important to know their physical properties by linking with their mechanical and bioactive properties. In addition to its well-behaviors on inhibition zone against bacterial occurrences, it can be concluded that increasing Ag_20 would increase the gamma-ray attenuation properties of studied bioactive glass system. However, further efforts are recommended to see the availability, limitations, advantages and disadvantages of maximum Ag_20 additive amount in bioactive glass structure.

Data availability statement

The raw/processed data required to reproduce these findings can be made available upon a request.

Declaration of Competing Interest

The authors declare that they have no known competing financial interests or personal relationships that could have appeared to influence the work reported in this paper.

Acknowledgment

The authors thank for the scholar and research grant under Universiti Putra Malaysia, Taif University Researchers Supporting Project number (TURSP-2020/12), Taif University, Saudi Arabia and Deanship of Scientific Research at King Khalid University for financial support through General Research Project under grant number (G.R.P/81/42).

REFERENCES

[1] Hench LL, Splinter RJ, Allen WC, Greenlee TK. Bonding mechanisms at the interface of ceramic prosthetic materials. J Biomed Mater Res 1971;5:117–41.
[2] Bergmann C, Lindner M, Zhang W, Koczur K, Kirsten A, Telle R, et al. 3D printing of bone substitute implants using calcium phosphate and bioactive glasses. J Eur Ceram Soc 2010;30:2563–7.
[3] Sergi R, Bellucci D, Cannillo V. A review of bioactive glass/natural polymer composites: state of the art. Materials 2020;13:5560.
[4] Hench LL, Xynos ID, Polak JM. Bioactive glasses for in situ tissue regeneration. J Biomater Sci Polym Ed 2004;15:543–62.
[5] Elgayar I, Aliev AE, Boccaccini AR, Hill RG. Structural analysis of bioactive glasses. J Non-Cryst Solids 2005;351:173–83.
[6] Hesaraki S, Gholami M, Vazehrad S, Shahrabi S. The effect of Sr concentration on bioactivity and biocompatibility of sol–gel derived glasses based on $CaO–SrO–SiO_2–P_2O_5$ quaternary system. Mater Sci Eng C 2010;30:383–90.
[7] Khiri MZA, Matori KA, Zaid MHM, Abdullah AC, Zainuddin N, Jusoh WNW, et al. Soda lime silicate glass and clam Shell act as precursor in synthesize calcium fluoroaluminosilicate glass to fabricate glass ionomer cement with different ageing time. J Mater Res Technol 2020;9:6125–34.
[8] Naresh P, Narsimlu N, Srinivas C, Shareefuddin M, Kumar KS. Ag_2O doped bioactive glasses: an investigation on the antibacterial, optical, structural and impedance studies. J Non-Cryst Solids 2020;549:120361.
[9] Mann KS, Mann SS. Py-MLBUF: development of an online-platform for gamma-ray shielding calculations and investigations. Ann Nucl Energy 2021;150:107845.

[10] Kilicoglu O, Tekin HO. Bioactive glasses and direct effect of increased K_2O additive for nuclear shielding performance: a comparative investigation. Ceram Int 2020;46:1323–33.
[11] Al-Buriahi MS, Sriwunkum C, Arslan H, Tonguc BT, Bourham MA. Investigation of barium borate glasses for radiation shielding applications. Appl Phys A 2020;126:1–9.
[12] Al-Buriahi MS, El-Agawany FI, Sriwunkum C, Akyıldırım H, Arslan H, Tonguc BT, et al. Influence of Bi_2O_3/PbO on nuclear shielding characteristics of lead-zinc-tellurite glasses. Phys B Condens Matter 2020;581:411946.
[13] Al-Hadeethi Y, Sayyed MI, Al-Buriahi MS. Bioactive glasses doped with TiO_2 and their potential use in radiation shielding applications. Ceram Int 2020;46:14721–32.
[14] Rahman NAA, Matori KA, Zaid MHM, Zainuddin N, Ab Aziz S, Khiri MZA, et al. Fabrication of alumino-silicate-fluoride based bioglass derived from waste clam shell and soda lime silica glasses. Results Phys 2019;12:743–7.
[15] Tekin HO, Kavaz E, Altunsoy EE, Kilicoglu O, Agar O, Erguzel TT, et al. An extensive investigation on gamma-ray and neutron attenuation parameters of cobalt oxide and nickel oxide substituted bioactive glasses. Ceram Int 2019;45:9934–49.
[16] Mostafa AMA, Zakaly HM, Pyshkina M, Issa SA, Tekin HO, Sidek HAA, et al. Multi-objective optimization strategies for radiation shielding performance of BZBB glasses using Bi_2O_3: a FLUKA Monte Carlo code calculations. J Mater Res Technol 2020;9:12335–45.
[17] Boukhris I, Kebaili I, Al-Buriahi MS, Alalawi A, Abouhaswa AS, Tonguc B. Photon and electron attenuation parameters of phosphate and borate bioactive glasses by using Geant4 simulations. Ceram Int 2020;46:24435–42.
[18] Boukhris I, Alalawi A, Al-Buriahi MS, Kebaili I, Sayyed MI. Radiation attenuation properties of bioactive glasses doped with NiO. Ceram Int 2020;46:19880–9.
[19] Alalawi A, Al-Buriahi MS, Rammah YS. Radiation shielding properties of PNCKM bioactive glasses at nuclear medicine energies. Ceram Int 2020;46:15027–33.
[20] Al-Hadeethi Y, Al-Buriahi MS, Sayyed MI. Bioactive glasses and the impact of Si_3N_4 doping on the photon attenuation up to radiotherapy energies. Ceram Int 2020;46:5306–14.
[21] Kilicoglu O. Characterization of copper oxide and cobalt oxide substituted bioactive glasses for gamma and neutron shielding applications. Ceram Int 2019;45:23619–31.
[22] Agar O, Khattari ZY, Sayyed MI, Tekin HO, Al-Omari S, Maghrabi M, et al. Evaluation of the shielding parameters of alkaline earth based phosphate glasses using MCNPX code. Results Phys 2019;12:101–6.
[23] Elazaka AI, Zakaly HM, Issa SA, Rashad M, Tekin HO, Saudi HA, et al. New approach to removal of hazardous Bypass Cement Dust (BCD) from the environment: $20Na_2O$-$20BaCl_2$-$(60-x)B_2O_3$-(x) BCD glass system and Optical, mechanical, structural and nuclear radiation shielding competences. J Hazard Mater 2021;403:123738.
[24] Battistoni G, Cerutti F, Fasso A, Ferrari A, Muraro S, Ranft J, et al. The FLUKA code: description and benchmarking. In: AIP Conference proceedings. 896; 2007. p. 31–49.
[25] Al-Buriahi MS, Arslan H, Tonguç BT. Mass attenuation coefficients, water and tissue equivalence properties of some tissues by Geant4, XCOM and experimental data. Indian J Pure Appl Phys 2019;57:433–7.
[26] Al-Buriahi MS, Tekin HO, Kavaz E, Tonguc BT, Rammah YS. New transparent rare earth glasses for radiation protection applications. Appl Phys A 2019;125:1–9.
[27] Zakaly HM, Saudi HA, Issa SA, Rashad M, Elazaka AI, Tekin HO, et al. Alteration of optical, structural, mechanical durability and nuclear radiation attenuation properties of barium borosilicate glasses through BaO reinforcement: experimental and numerical analyses. Ceram Int 2021;47:5587–96.
[28] Singh VP, Badiger NM. Effective atomic weight, effective atomic numbers and effective electron densities of hydride and borohydride metals for fusion reactor shielding. J Fusion Energy 2014;33:386–92.
[29] Sayyed MI, Akyildirim H, Al-Buriahi MS, Lacomme E, Ayad R, Bonvicini G. Oxyfluoro-tellurite-zinc glasses and the nuclear-shielding ability under the substitution of AlF 3 by ZnO. Appl Phys A 2020;126:1–12.
[30] Ai T, Wang F, Feng X, Ruan M. Microstructural and mechanical properties of dual Ti_3AlC_2–Ti_2AlC reinforced TiAl composites fabricated by reaction hot pressing. Ceram Int 2014;40:9947–53.
[31] Mostafa AMA, Issa SA, Zakaly HM, Zaid MHM, Tekin HO, Matori KA, et al. The influence of heavy elements on the ionizing radiation shielding efficiency and elastic properties of some tellurite glasses: theoretical investigation. Results Phys 2020;19:103496.